Journal of Sound and Vibration (1999) **228**(4), 773–792
Article No. jsvi.1999.2443, available online at http://www.idealibrary.com on IDEAL®

VIBRATION CONTROL OF A STRUCTURE BY USING A TUNABLE ABSORBER AND AN OPTIMAL VIBRATION ABSORBER UNDER AUTO-TUNING CONTROL

K. NAGAYA, A. KURUSU, S. IKAI AND Y. SHITANI
Department of Mechanical Engineering, Gunma University, Kiryu, Gunma 376-8515, Japan

(*Received* 16 *April* 1998, *and in final form* 1 *June* 1999)

Vibrations of machines and structures vanish perfectly at a certain frequency when they have a vibration absorber without damping. But if forced frequencies vary from the anti-resonance frequency, their vibration amplitudes increase significantly. Then the absorber without damping cannot be applied to the structure subjected to variable frequency loads or the loads having high-frequency components. The present article discusses a method of vibration control of a structure by using the vibration absorber without damping. In this method, a variable stiffness vibration absorber is used for controlling a principal mode. The stiffness is controlled by the microcomputer under the auto-tuning algorithm for creating an anti-resonance state. The optimal vibration absorber with damping is also utilized for controlling higher modes. The analyses and the algorithm for the auto-tuning control are developed. A method to obtain optimal parameters has been presented for the vibration absorber which controls higher modes. In order to validate the control method and the analysis, experimental tests have been carried out.

1. INTRODUCTION

Various vibration absorbers and dampers have been presented in a number of papers [1–4]. Recently, complicated phenomena of vibration absorbers such as non-linear vibrations have been discussed in references [5, 6]. Vibration absorbers have been used for suppressing vibrations of various structures [7, 8], and machines such as offshore platform [9], valves [10], multi-stage pumps [11], and shock absorbers of machines [12]. The absorbers as just mentioned are the vibration control elements for passive control, so in the design, maximum amplitudes of the vibrating body are minimized in a wide frequency zone by using optimal absorber parameters. Recently, active and active/passive vibration absorbers have been discussed [13–15] in which rigidity and damping are varied by using actuators. Najet *et al.* [16] gave an interesting tunable absorber for a two-degree-of-freedom system in which the optimal poles were given by the use of time-delay feedback. Recently, Sun *et al.* [17] gave a survey of passive, adaptive and active tuned absorbers.

0022-460X/99/490773 + 20 $30.00/0

Vibrations of a mass having a vibration absorber without damping vanish perfectly when the frequency of a sinusoidal force acting on the mass is equal to the natural frequency of the absorber. Since the phenomenon is just opposite to the resonance, the phenomenon is called "anti-resonance", and the frequency in which the vibration amplitude becomes minimum is called "anti-resonance frequency" in the present paper. When the forced frequency is different from the anti-resonance frequency, the vibration amplitude of the mass increases signifcantly. For the reason as just mentioned, the absorber using the principle has not been used in practical problems. In the absorber, if the stiffness of the absorber is tunable, vibrations of the mass can be suppressed perfectly from a theoretical stand point. The principle has been used for controlling vibrations for a rigid body [17, 18] by use of the tunable vibration absorber. The methods in references [16–18] are applicable in case of a rigid body and sinusoidal exciting force.

In practical structures, exciting forces have complicated waves with respect to time, which are different from the sinusoidal waves in general. This implies that the forces involve higher frequency components, and hence the higher vibration modes are generated for flexible structures. The tunable vibration absorbers for the rigid body under sinusoidal forces cannot be applied directly to such a problem. Then all resonance peaks in the frequency domain have to be suppressed in the design of absorbers for flexible structures. In order to reduce resonance peaks, and to have flat response curve in a frequency domain, vibration absorbers with damping have been widely used [7–15]. However, the amplitudes at a low-frequency region within the first resonance frequency are greater than the displacement due to the static load whose intensity is equal to the amplitude of vibration load. Hence, the maximum amplitude ratio in the frequency domain is greater than unit [the amplitude of displacement due to a vibration load with amplitude P/(the displacement due to the static load with intensity P) > 1] when the vibration absorbers with damping are used. In addition, the number of vibration absorbers has to be equal to that of control modes. Hence, many absorbers are required.

In the present article, a method of vibration control for structures has been presented with consideration of higher modes of vibrations. In our method, the principal vibration mode is controlled by use of auto-tuning anti-resonance control of the tunable vibration absorber without damping, and the higher modes are suppressed by the optimal vibration absorber with a magnetic damper. Theoretical results under the control have been presented. In order to validate the present control method and analyses, experimental tests have been carried out.

2. RESPONSE OF A STRUCTURE WITH VIBRATION ABSORBERS

The purpose of this paper is to suppress vibrations of structures with consideration of higher modes. When a structure is excited by a cyclic exciting force whose principal frequency is smaller than the first resonance frequency, the vibration amplitude with the forced frequency is significant, but the components of higher frequencies are also involved in the amplitude. When an ordinary vibration absorber with damping is used, vibration amplitudes in a low-frequency region

cannot be suppressed (the amplitude ratio is greater than unit). The tunable vibration absorber without damping suppresses vibrations for the principal mode, but it cannot suppress higher modes. In order to suppress vibrations in a wide frequency region, the present article proposes a system consisting of a tunable vibration absorber and a vibration absorber with a magnetic damper. The tunable absorber suppresses the principal mode, and the vibration absorber with the damper suppresses higher vibration modes. When the vibration absorbers with damping are used, the number of vibration absorbers has to be equal to that of the control modes in the usual design of absorbers. The vibrations of higher modes can be suppressed by small damping, because a damping force is in proportion to the vibrating speed. The present authors presented a method for suppressing higher modal vibrations by using the fewer number of vibration absorbers with consideration of the damping phenomena just mentioned [19]. In the method, the absorbers control higher modes whose number is greater than the number of vibration absorbers. The method is used to design the absorber in the present article.

Figure 1 shows the geometry of the structure with the absorbers in which one of the absorber has no damping (the tunable absorber for anti-resonance is called absorber 1), and the other has the magnetic damper (the absorber for higher modes is called absorber 2). The locations of the absorbers are important, because the system parameters vary with the stiffness of the tunable absorber. The optimal parameters of the vibration absorber with damping vary with the system parameters. This implies that both the tunable absorber and the vibration absorber with damping cannot be used simultaneously. In order to use the absorber for higher modes, the tunable absorber (absorber 1) lies on the nodal point of the second mode of the structure, and so the motion of absorber 1 does not affect the second mode, because, the second mode vibration is not generated due to the excitation at the second nodal point. Absorber 2 lies at the anti-nodal point of the second mode. The motion of absorber 2 due to the second modal vibration also

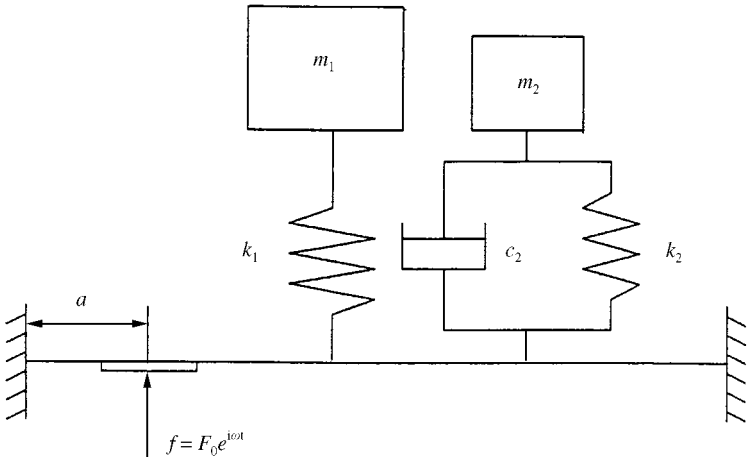

Figure 1. Geometry of the beam with vibration absorbers.

does not affect the first mode (the phenomena will be clarified in the analysis). Then absorber 2 can be designed without consideration of absorber 1, and the constant optimal parameters of the absorber are applicable. For the first mode, since absorber 2 is not laid on the nodal point of the first mode, it affects the first modal vibration of course, but its effect can be involved in the auto-tuning control of the first mode.

In order to indicate the validity of the present system, consider a simple beam with both built-in edges. The theoretical model is shown in Figure 1. The vibration response can be obtained by using the transfer matrix method whose nature has been discussed in references [20, 21]. The matrix equation between the jth and $(j+1)$th element of the beam is

$$V_j^L = F_j V_{j-1}^R, \tag{1}$$

where

$$V_j = [w\ \phi\ T\ Q\ 1]^{\mathrm{T}}$$

$$F_j = \begin{bmatrix} 1 & -L_j & \dfrac{L_j^2}{2EI_j} & \dfrac{L_j^3}{6EI_j} & 0 \\ 0 & 1 & \dfrac{-L_j}{EI_j} & \dfrac{-L_j^2}{2EI_j} & 0 \\ 0 & 0 & 1 & L_j & 0 \\ 0 & 0 & 0 & 1 & 0 \\ 0 & 0 & 0 & 0 & 1 \end{bmatrix} \tag{2}$$

and where R denotes the right side, L the left side, w the displacement of the beam, ϕ the bending slope, T the bending moment, Q the shearing force, L_j the element length and EI_j the flexural rigidity. The equation between the right side R and the left side L at an arbitrary point j is

$$V_j^R = P_j V_j^L, \tag{3}$$

where

$$P_j = \begin{bmatrix} 1 & 0 & 0 & 0 & 0 \\ 0 & 1 & 0 & 0 & 0 \\ 0 & 0 & 1 & 0 & 0 \\ M_j\omega^2 & 0 & 0 & 1 & f_j \\ 0 & 0 & 0 & 0 & 1 \end{bmatrix}_j \tag{4}$$

and where M_j is the element mass at the point j, f_j the load amplitude acting on the point j, and ω the forced angular frequency.

The equation of motion of the vibration absorber is

$$m_2 \frac{\mathrm{d}^2 u}{\mathrm{d}t^2} + c_2\left(\frac{\mathrm{d}u}{\mathrm{d}t} - \frac{\mathrm{d}w}{\mathrm{d}t}\right) + k_2(u - w) = 0, \tag{5}$$

where m_2 is the mass, k_2 the spring constant, c_2 the damping coefficient, and u the displacement of the mass of the vibration absorber, respectively. Substituting $w = W_0 e^{\mathrm{i}\omega t}$, $u = U_0 e^{\mathrm{i}\omega t}$ into equation (5), one obtains

$$Q = B_2(\omega) m_2 \omega^2, \tag{6}$$

where

$$B_2(\omega) = \frac{p_2^2 + 2\mu\omega\mathrm{i}}{p_2^2 - \omega^2 + 2\mu\omega\mathrm{i}}, \tag{7}$$

$$2\mu = c_2/m_2, \quad p_2^2 = k_2/m_2, \quad i = \sqrt{-1}.$$

Hence, the point transfer matrix at absorber 2 is

$$P_j = \begin{bmatrix} 1 & 0 & 0 & 0 & 0 \\ 0 & 1 & 0 & 0 & 0 \\ 0 & 0 & 1 & 0 & 0 \\ (M_j + B_2 m_2)\omega^2 & 0 & 0 & 1 & 0 \\ 0 & 0 & 0 & 0 & 1 \end{bmatrix}. \tag{8}$$

The size and weight of absorber 1 are not small, and so a rotary inertia must be considered. The point transfer matrix with such consideration is

$$P_j = \begin{bmatrix} 1 & 0 & 0 & 0 & 0 \\ 0 & 1 & 0 & 0 & 0 \\ 0 & -J\omega^2 & 1 & 0 & 0 \\ (M_j + B_1 m_1)\omega^2 & 0 & 0 & 1 & 0 \\ 0 & 0 & 0 & 0 & 1 \end{bmatrix}_j, \tag{9}$$

where J is the moment of inertia of absorber 1, and where

$$B_1(\omega) = \frac{p_1^2}{p_1^2 - \omega^2}. \tag{10}$$

Since both ends of the beam are built-in, the boundary conditions are

$$(w)_0 = (\phi)_0 = (\mathrm{w})_N = (\phi)_N = 0, \tag{11}$$

where 0 denotes the left end, and N the number of the point at the right end of the beam, from which one obtains the state variables at point 0:

$$Q_0 = \frac{a_{25}a_{13} - a_{23}a_{15}}{\det}, \quad T_0 = \frac{a_{25}a_{14} - a_{24}a_{15}}{\det},$$

$$\det = a_{24}a_{13} - a_{23}a_{13},$$

where a_{ij} is the element of ith row and jth column of the transfer matrix $T_N = P_N F_N \cdots P_1 F_1$. The state vector V_n at the right side R on an arbitrary point n is obtained by the following equation:

$$V_n = P_n F_n \cdots P_1 F_1 V_0. \tag{12}$$

Numerical calculations are carried out for the beam with vibration absorbers used in the experiment as mentioned below. An aluminum beam with channel shape is used. Table 1 shows the dimensions of the beam. The dimensions for the variable stiffness absorber (see Figure 2) used in the calculation are also depicted in Table 2. The nodal point of the second mode is calculated as $x = 46$ cm from the left end of the beam where the auto-tuning absorber is attached (hereafter, the point is called as point A). Numerical calculations are carried out under the assumption that the sinusoidal force with amplitude 10 N acts on the point measured from 24·5 cm from the left end of the beam. Figure 3 depicts the compliance versus the forced angular frequency at point A. The resonance frequency of the beam varies with the stiffness of the absorber (the natural frequency of the absorber). The anti-resonance frequency also varies with the stiffness of the absorber. However, since the variable stiffness absorber lies on the nodal point of the second mode, the second resonance frequency has no dependence on the stiffness of the absorber. This implies that absorber 2 can be designed without consideration of stiffness variation of absorber 1. The total mass of the absorber is large, and so the resonance peaks of higher modes more than the third mode are significantly small in comparison with the first two peaks. If the anti-resonance frequency is tuned to

TABLE 1

Dimensions of the beam

Material	Aluminum
Shape of the cross-section	Channel
Size of the cross-section	$21{\cdot}5 \times 60{\cdot}4 \times 3{\cdot}3$ (mm)
Length of the beam	980 (mm)
Young's modulus	$7{\cdot}06 \times 10^{10}$ (N/m^2)
Density	$2{\cdot}7 \times 10^3$ (kg/m^3)
Total mass of the beam	0·845 (kg)
Moment of the cross-section	$1{\cdot}2 \times 10^{-8}$ (m^4)
Mass of the attached plate at the forcing point	0·5 (kg)

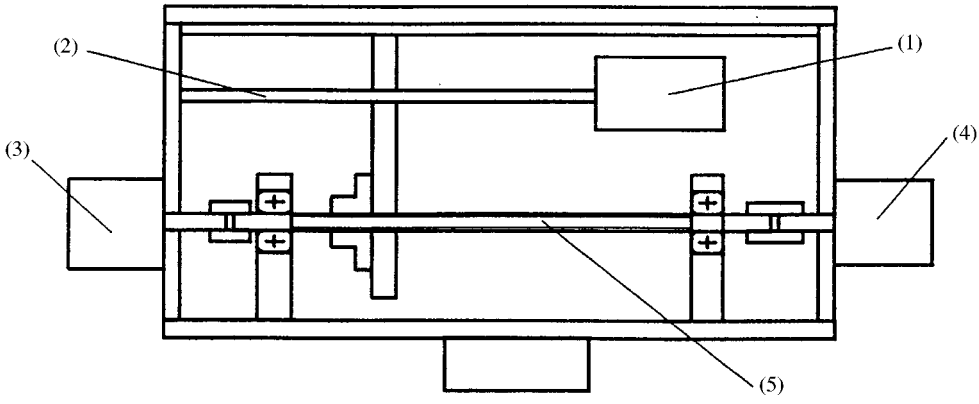

Figure 2. Geometry of the anti-resonance absorber (variable stiffness absorber)

TABLE 2

Dimensions of the variable stiffness absorber for anti-resonance control

Attached mass at the tip of beam	0·6 (kg)
Eigenfrequency of the absorber	13–29 (Hz) (variable)
Spring of the absorber	Beam made of a stainless bar
Total mass of the absorber	4·23 (kg)

be the principal frequency of the forced load, the vibration amplitude of the first mode of the beam becomes zero when there is no damping. Since the present system has a damper in absorber 2 for suppressing higher modes, the first modal vibration does not become zero, and so the small damping is desirable for absorber 2.

From Figure 3, it is ascertained that the combination of the tunable absorber and the absorber with damping is able to control vibrations.

3. METHOD OF AUTO-TUNING OF ABSORBER 1 FOR THE ANTI-RESONANCE CONTROL

In the present paper, the first modal vibration is controlled by the tunable (variable stiffness) absorber under the anti-resonance control. Figure 2 shows the geometry of absorber 1 for the anti-resonance (variable stiffness absorber). The variable stiffness absorber consists of the mass, beam, rotary encoder, motor and ball screw as shown in Figure 2. In the absorber, the spring constant at mass (1) varies by moving the middle support of beam (2). The moving support consists of a Teflon plate with a hole in which a circular stainless bar is inserted. The ball nut is connected to the plate. Hence, the middle support moves when the motor rotates.

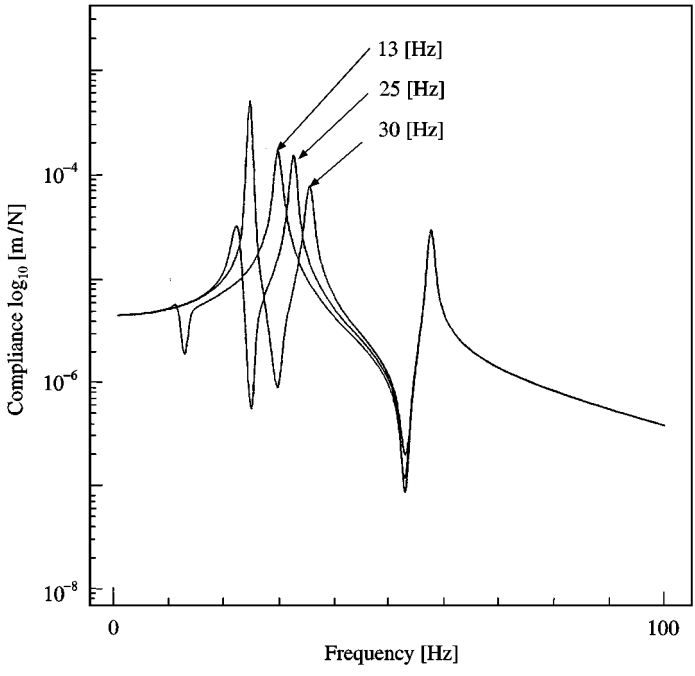

Figure 3. Theoretical response of the beam for various values of the rigidity of the anti-resonance vibration absorber.

The angle of rotation of the motor is detected by the rotary encoder (3) attached to the ball screw.

In order to have the anti-resonance state, a method of auto-tuning with two steps is presented. The acceleration signal is measured by the acceleration sensor. It is converted into the displacement signal by using the integration circuits. The displacement signal is input to the digital signal processor (DSP). In the first step control, the principal frequency is calculated, and the angle of rotation of the motor is calculated. The motor is rotated until the calculated angle, where the angle of rotation is detected by the rotary encoder. If the theoretical anti-resonance frequency coincides with the actual frequency, one obtains the anti-resonance state by using the theoretical expression. At the anti-resonance frequency, the response curve is sharp as shown in Figure 3, and so a few theoretical error has considerable effects on the amplitude of the beam. Hence, it is difficult to create the anti-resonance state by the control based on the theoretical analysis. The theoretical analysis can be applied for obtaining approximate rotation angles of the motor. Then the second step (precise auto-tuning) control is required.

The second step auto-tuning control is performed as follows. The support of the absorber beam is moved a little from the position settled by the control based on the analysis. The vibration amplitude after the support movement is compared with that before the movement, and the support is moved in the direction where the vibration amplitude decreases. The support movement (the rotation angle of the motor) is decreased with decreasing values of the vibration amplitude of the beam.

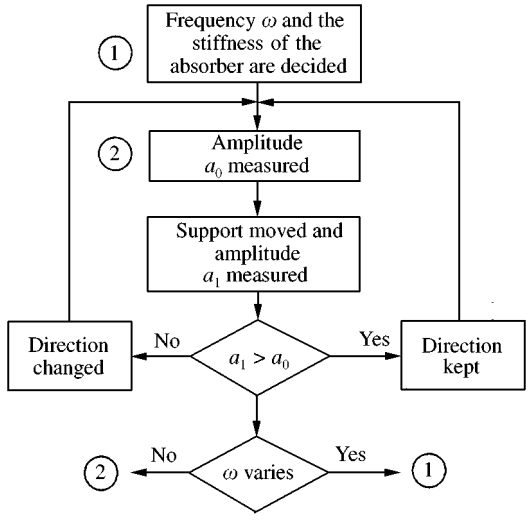

Figure 4. Flow chart of control of the anti-resonance vibration absorber.

By repeating the control, one obtains the anti-resonance state automatically by using the DSP. Figure 4 shows the algorithm of this control.

4. METHOD TO OBTAIN OPTIMAL PARAMETERS OF VIBRATION ABSORBER 2

When the anti-resonance control is performed, the first mode vibration is controlled to be significantly small. However, higher modes cannot be controlled. In order to control higher modes, the damper with large damping is desirable, but it affects the first mode. This implies that, small damping is desirable for the control of higher modes. Hence, the optimal vibration absorber is used for the higher modes. When the optimal vibration absorbers is used, vibrations of higher modes are suppressed by use of the optimal damping coefficient. The damping is not so large, because the mass of the absorber damps vibrations. In the usual design of vibration absorbers, the number of absorbers has to be equal to that of the control modes. For the problem, the present author proposed a method of control of higher modes by use of the small number of absorbers. We controlled the first five modes successfully by use of only three absorbers in the problem of plate vibrations [19]. In the present article, the method is also applicable to the design of the absorber.

The effect of the absorber is large when the absorber lies on the anti-nodal point where the mode shape has a maximum value. Then absorber 2 lies near the anti-nodal point of the second mode (The point was calculated as $x = 65$ cm measured from the left end of the beam by using the analysis mentioned above. Hereafter, the point is called point B). The vibrations of higher modes can be suppressed by small damping, because the damping force is in proportion to the vibrating speed. Then the absorber can control not only the second mode but also higher modes due to the damping called "fluid damper effect". Usually, the fluid

damper effects are not considered in the design of vibration absorbers. However, when higher modes are considered, the optimal absorber parameters are different from those of ordinary absorbers [19]. In the present article, absorber 2 is designed with consideration of higher modes. In order to have the optimal parameters of the absorber, the frequency response curve in higher modes except the region of the first mode (which is controlled by the anti-resonance control) is considered. The frequency response curve near higher peaks is divided into n-pieces for n-higher peaks in the considered region. Each divided curve is integrated with respect to the frequency in the considered frequency region from Ω_{1i} to Ω_{2i} for ith piece. Their summation is taken to be a cost function

$$W_p = \sum_{i=1}^{n} \int_{\Omega_{1i}}^{\Omega_{2i}} f(m_2, k_2, c_2, \omega) \mathrm{d}\omega, \tag{13}$$

where $f(m_2, k_2, c_2, \omega)$ is the vibration amplitude of displacement at the considered point in the beam. Numerical values of $f(m_2, k_2, c_2, \omega)$ is calculated by equation (12). Hence, one obtains the values of the cost function W_p by use of the numerical integration scheme. When we consider one absorber, the parameters of the absorber are m_2, k_2 and c_2. The optimal parameters can be obtained by the iterations of the following expression:

$$X_q = X_q - \eta_q \frac{\partial W_p}{\partial X_q} \quad (q = 1, 2, 3) \tag{14}$$

By repeating the calculation of equation (14), one obtains the optimal parameters $m_2 = X_1$, $k_2 = X_2$ and $c_2 = X_3$ which make the cost function W_p minimum. The method as just mentioned has advantages, because it controls higher modes by using the fewer number of absorbers. All higher modes more than the second mode will be controlled by using the present method. There is no guarantee that equation (14) will converge to the truly optimal solution, so that the calculation of equation (14) is performed for some initial values. The optimal values are decided when the solutions converge to the same value.

Table 3 depicts the calculated optimal values of the absorber for the present beam. One example of initial values (before the optimization) are also shown in the

TABLE 3

Dimensions of the absorber for higher modes

	Initial values	Optimal values
Spring constant	10^4 (N/m)	$2{\cdot}51 \times 10^4$ (N/m)
Damping coefficient	10 (N s/m)	9·07 (N s/m)
Attached mass	0·2 (kg)	0·205 (kg)
Total mass of the absorber	0·327 (kg)	

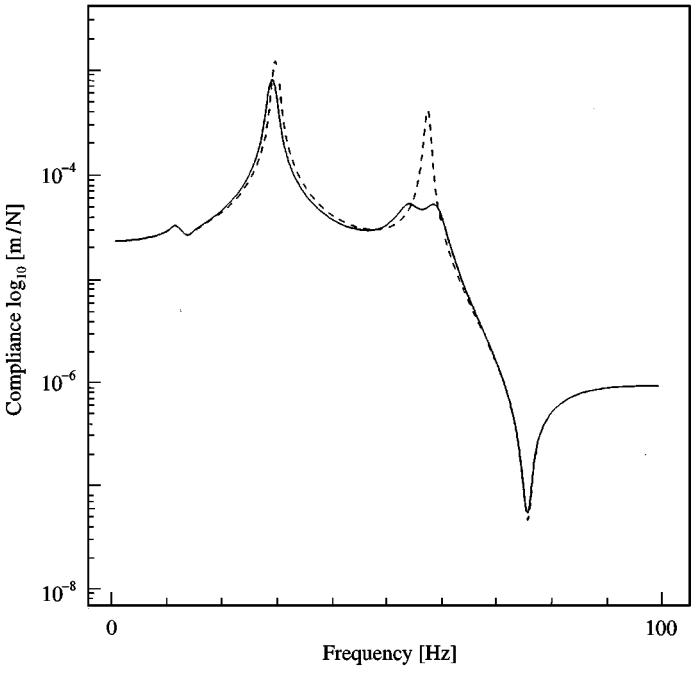

Figure 5. Theoretical response of the beam with optimal vibration absorbers for the second mode. ----- not optimized; —— optimized.

table. By using the values, the compliance of the beam at point B are calculated. The results are depicted in Figure 5. There is a large peak at the second resonance frequency when using the initial values before the optimization (see the dotted line), while the second resonance peak is suppressed when using the optimal values (see the solid line). Then the present method is applicable for designing the vibration absorber with the damper. Since the variable stiffness absorber lies on the nodal point of the second mode, the effect of variation of the tunable absorber on the second mode is almost zero in the figure. Hence, absorber 2 can be designed without considering variations of tunable absorber 1, and fixed parameters are applicable for the absorber 2. The tunable absorber also affects the modes greater than the third mode. But, although the damping effect varies with the stiffness of tunable absorber, the higher modes are suppressed by the fluid damper effects of course.

5. EXPERIMENTS

In order to validate the present control method and analyses, experimental tests have been carried out for the same model mentioned in the numerical calculation. Figure 6 illustrates the geometry of the control system. A magnetic damper is used in absorber 2. The rectangular aluminum plate conductor is inserted between two permanent magnets in which the N-pole of one magnet faces the S-pole of the other as shown in Figure 7. When the plate conductor vibrates, the magnetic force is generated. The force gives the damping which is in proportion to the velocity of the

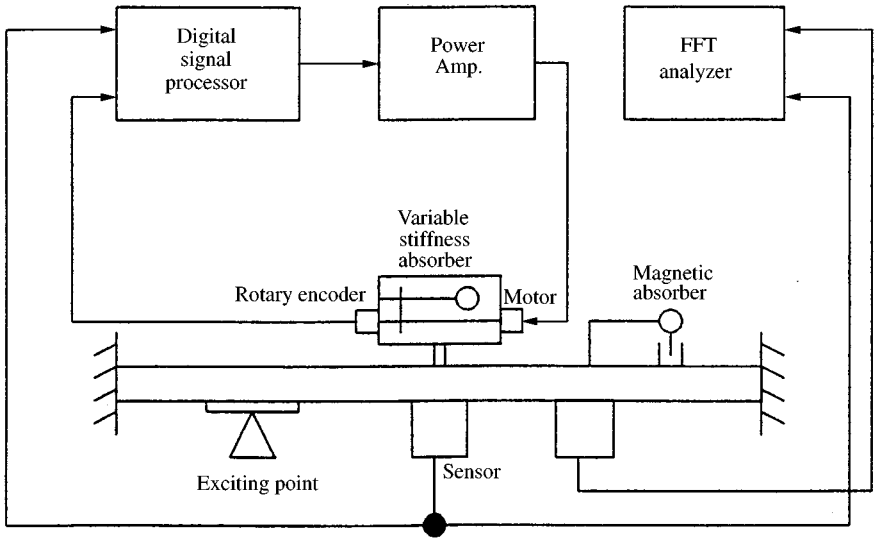

Figure 6. Geometry of the control system.

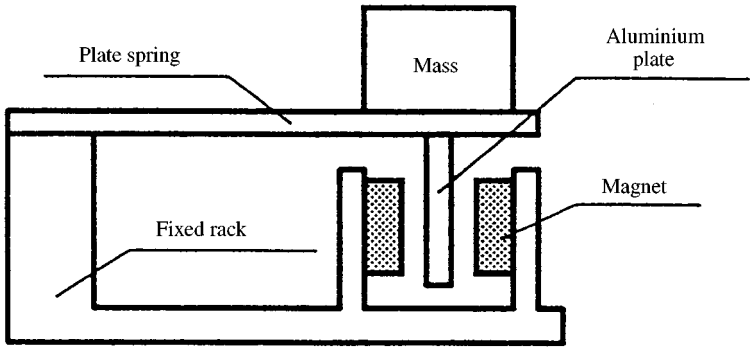

Figure 7. Geometry of the magnetic vibration absorber for higher modes.

plate conductor. The damping coefficient can be varied by adjusting the air gap between the magnets, hence one obtains the optimal damping coefficient shown in Table 3. The analysis of damping coefficients was reported in our previous report [3]. The spring constant of the absorber is also varied by adjusting the length of the plate spring shown in Figure 7. Then the optimal values of the mass and the spring constant in Table 3 are settled. The second resonance frequency has no dependence on the variation of the stiffness of the auto-tuning absorber (anti-resonance absorber) as shown in Figure 3, so the absorber with constant parameters is applicable of course as mentioned above. The first step control for obtaining the anti-resonance state requires the relationship between the eigenfrequency of the variable stiffness absorber and the length of the absorber beam measured from the tip mass. The relationship is non-linear as shown in Figure 8. Then the relationship is obtained as an expression by making use of the least-squares method. The solid line in Figure 8 illustrates the result obtained by the expression which is used in the first step control.

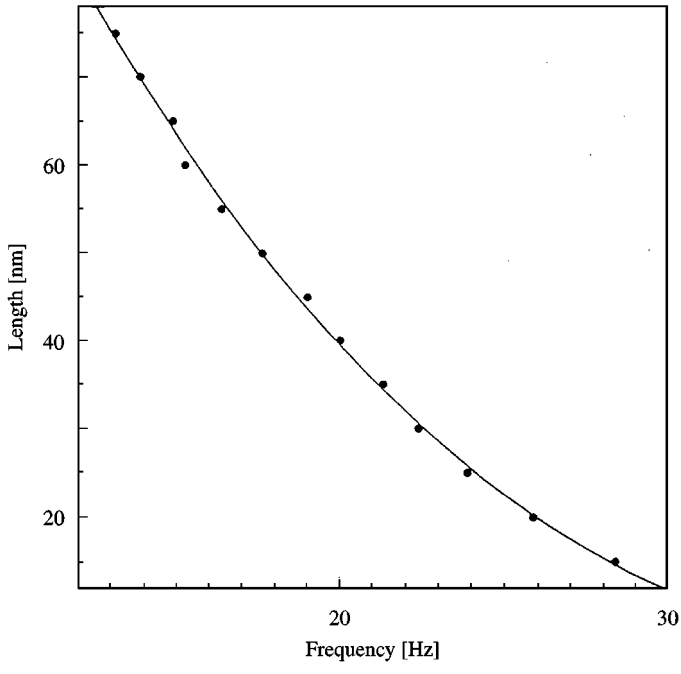

Figure 8. Relation between the length of the beam of the absorber and the natural frequencies.

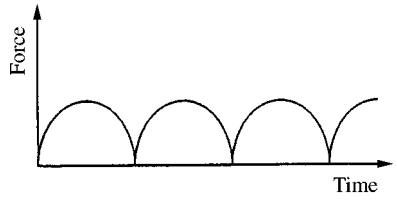

Figure 9. Shape of the exciting force generated by a magnet.

The acceleration sensors were attached at two points at $x = 46$ cm (point A) and $x = 65$ cm (point B) from the left end of the beam, and detected signals were input to the FFT analyzer as shown in Figure 6. The forced excitation was applied at the point $x = 24{\cdot}5$ cm from the left end of the beam by an electromagnet. Since the electromagnet generates attractive force only, and the force is in proportion to the square of the current, the exciting force becomes the square of half sine pulse as shown in Figure 9 under the sinusoidal input current. This implies that the force has various frequency components. Then the absorber to suppress higher modes is needed.

5.1. EXPERIMENTAL RESULTS WITHOUT VIBRATION ABSORBERS FOR HIGHER MODES IN CASE OF THE VARIABLE STIFFNESS ABSORBER BEING UNCONTROLLED

Experimental tests have been carried out for the beam with variable stiffness absorber, but without the vibration absorber for higher modes. Figure 10 illustrates

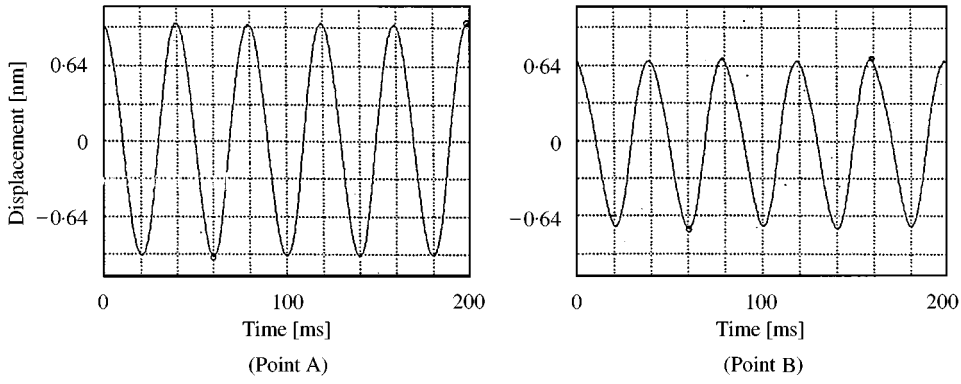

Figure 10. Experimental time-response curves for the beam without control and without absorber for higher modes in case of first resonance frequency excitation.

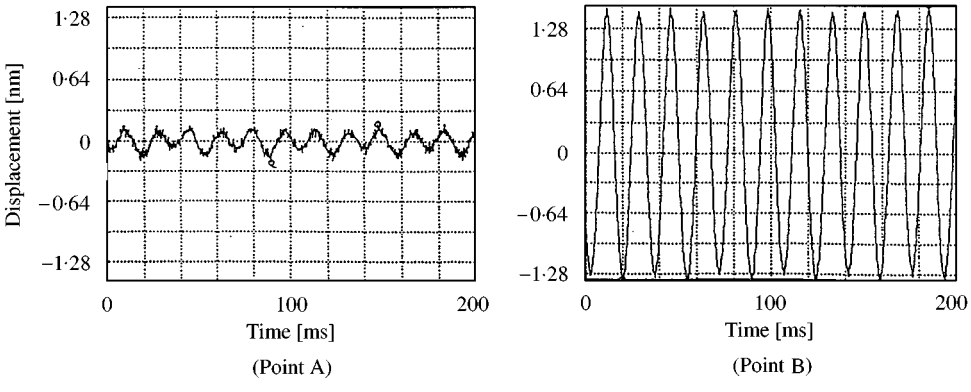

Figure 11. Experimental time-response curves for the beam without control and without absorber for higher modes in case of second resonance frequency excitation.

the experimental time response curve at both the points (points A and B) under the excitation of the first resonance frequency ($f = 25$ Hz). The response curves under the excitation of the second resonance frequency ($f = 58$ Hz) are also shown in Figure 11. The frequency spectrum are also shown in Figures 12 and 13, where the value (dB) illustrates $10 \log_{10} w$. In Figures 12 and 13, two typical peaks (the first and second modes) are observed. In addition, some of sub-harmonic and super-harmonic peaks due to the non-linear exciting force are also observed.

5.2. EXPERIMENTAL RESULTS WITH THE VIBRATION ABSORBER FOR HIGHER MODES IN CASE OF THE VARIABLE STIFFNESS ABSORBER BEING CONTROLLED

Figure 14 depicts the time-response curve of the beam with both the variable-stiffness absorber under the anti-resonance control and the magnetic absorber when the exciting load has the first resonance frequency ($f = 25$ Hz). The frequency spectrum in this case are shown in Figure 15. Figures 16 and 17 depict

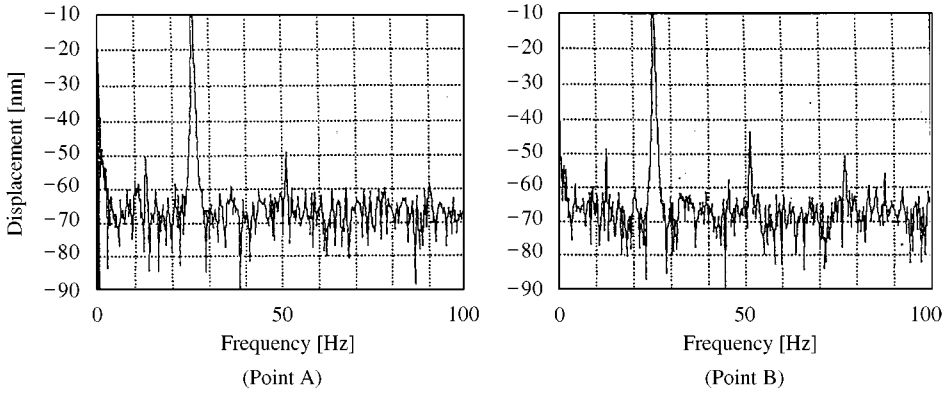

Figure 12. Experimental frequency spectrum for the beam without control and without absorber for higher modes in case of first resonance frequency excitation.

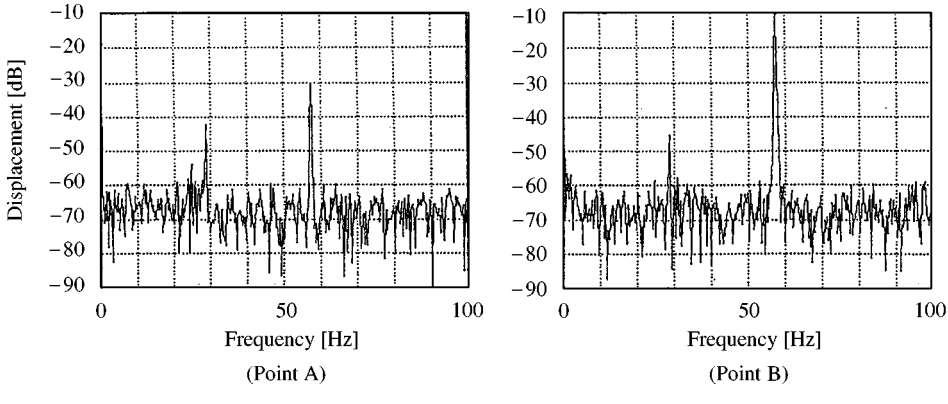

Figure 13. Experimental frequency spectrum for the beam without control and without absorber for higher modes in case of second resonance frequency excitation.

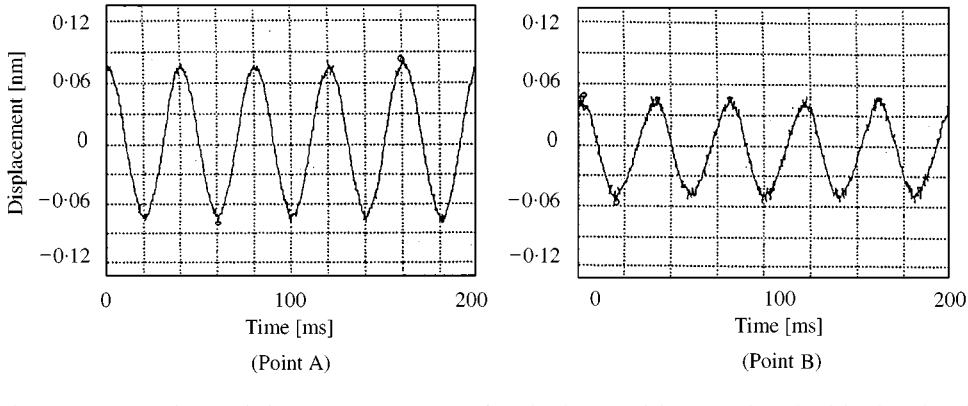

Figure 14. Experimental time-response curves for the beam with control and with absorber for higher modes in case of first resonance frequency excitation.

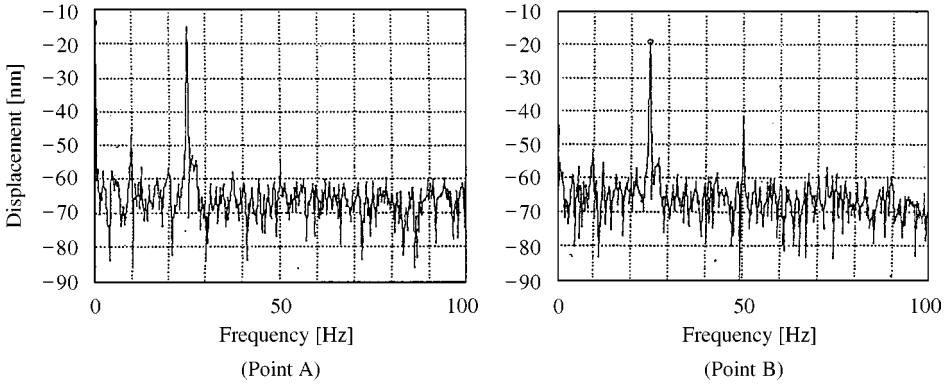

Figure 15. Experimental frequency spectrum for the beam with control and with absorber for higher modes in case of first resonance frequency excitation.

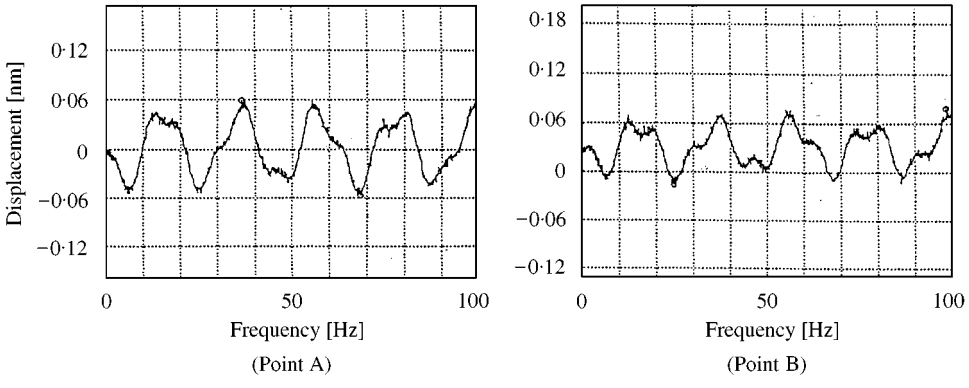

Figure 16. Experimental time-response curves for the beam with control and with absorber for higher modes in case of second resonance frequency excitation.

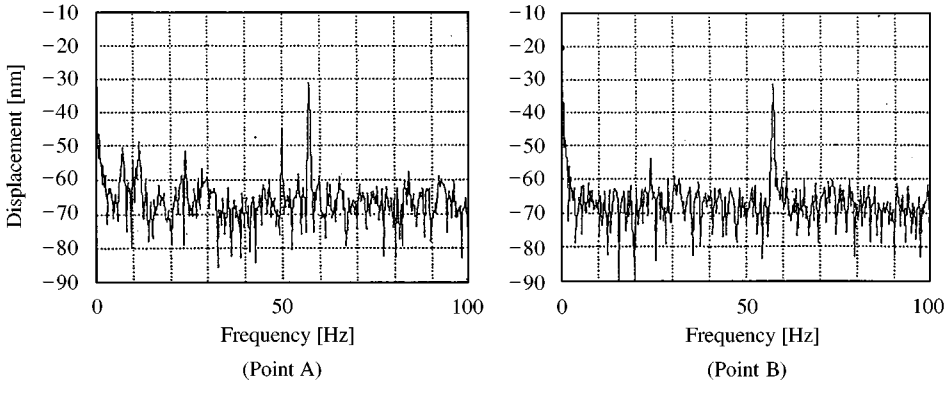

Figure 17. Experimental frequency spectrum for the beam with control and with absorber for higher modes in case of second resonance frequency excitation.

the results under the control subjected to second resonance frequency excitation. The amplitude under the present control at the resonance frequency is suppressed within only 8·6 per cent of the uncontrolled result (see Figure 10). Especially, sub-harmonic and super-harmonic motions are also supressed significantly as shown in Figure 15.

The present control is also applicable when the system parameters and forced frequency vary. In Figure 18, the result is shown when the forced frequency varies suddenly from the anti-resonance state. It shows that the amplitude of the beam increases with the variation of the forced frequency, but after about 2 s the anti-resonance state is created again by the auto-tuning control, and hence the amplitude is suppressed.

The frequency response at the point A of the beam is depicted by the solid line in Figure 19, where the anti-resonance states are created. Figure 20 also shows the response at the point B. In the figures, the dashed line is the result without control. The figures show that the vibration amplitudes under the present control are suppressed significantly in a wide frequency range involving first and second resonance frequencies. Especially, when using the usual vibration absorbers, the amplitudes for the low-frequency region are almost the same as those without control, because the effects of inertia force for low-frequency is small. Hence it is difficult to control amplitude ratios for low-frequencies less than one in the usual vibration absorbers or the PID active control. However, when the present method is used, the vibration amplitudes of the beam for the low-frequency region are significantly small. This is the advantage of using the present method.

In the present problem, since the first two peaks in the frequency response curve are significant, the higher modes greater than the third mode are not considered in the design of absorber 2 because the principal frequency of the exciting force is considered to be within 100 Hz (6000 rpm). In usual machines and structures, the principal frequencies are not large, so the effect of the first mode is significant, the second mode is the next, and components higher than the third mode are small

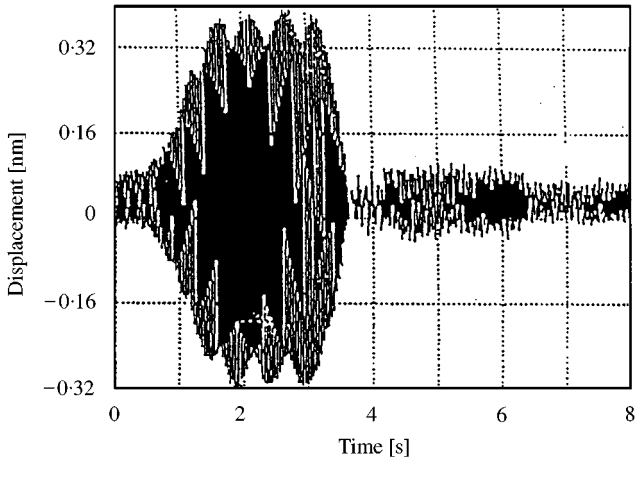

Figure 18. Experimental time response at point A of the beam with control and with absorber for higher modes when the frequency is changed.

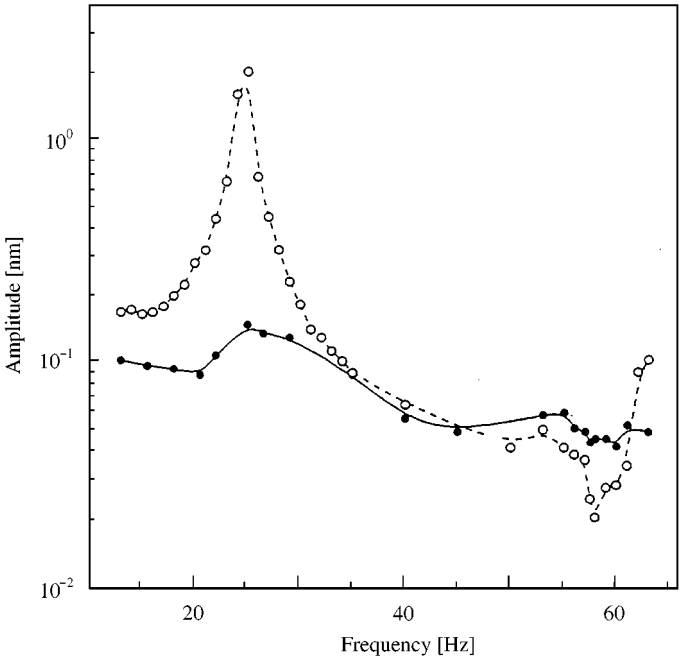

Figure 19. Frequency response at point A in the beam. —— with control; ----- without control.

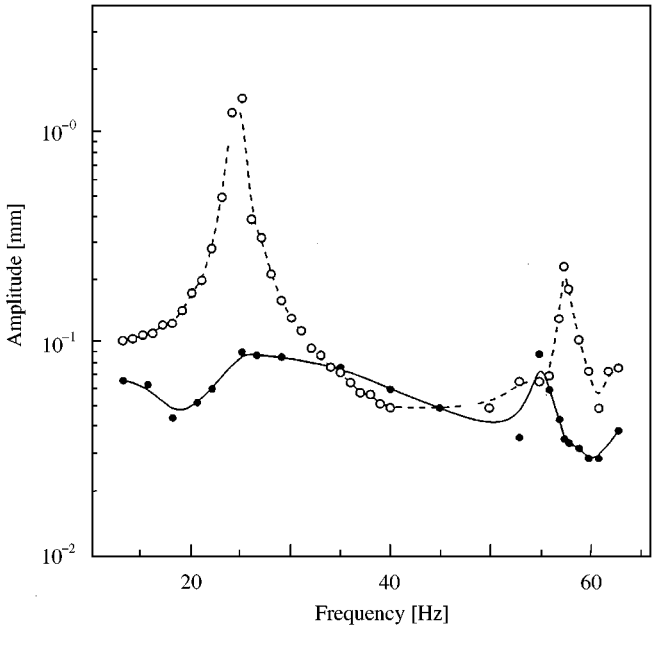

Figure 20. Frequency response at point B in the beam. —— with control; ----- without control.

even if the exciting force involves high-frequency components. Hence, higher modes may be suppressed by the damper effect of the second absorber as mentioned above.

6. CONCLUSION

A method of vibration control of structures has been presented. In the method, a variable stiffness absorber was presented for controlling vibrations of the first mode by using an auto-tuning anti-resonance control. The algorithm by use of a microcomputer was presented for the auto-tuning control. In order to control vibrations higher than the second mode, a vibration absorber with a damper was used, and its design method to obtain optimal parameters of the absorber was presented.

Experimental tests have been carried out for a flexible beam, and it is clarified that the vibrations can be controlled to be significantly small by use of the present method.

In the ordinary vibration absorbers, the amplitude ratio in the low-frequency region is greater than unit, while the present method enables one to reduce the amplitude ratio to 0·5. This is the essential advantage of using the present method. In addition, the number of vibration absorbers has to be equal to that of the control modes in the usual design method of absorbers. The absorber designed by the present method enables one to suppress vibrations of the higher modes by use of a fewer number of absorbers.

It is also clarified that the present method is applicable when the system parameters and forced frequencies with higher components vary during vibrations.

Although the variable stiffness absorber is controlled by the servo-motor, the vibration control is carried out based on the passive control. This implies that the control energy is significantly small in comparison with active controls.

Therefore, the present method has advantages over the previous methods.

REFERENCES

1. J. C. Snowdon, A. A. Wolf and R. L. Kerlin 1984 *The Journal of Acoustical Society of America* **75**, 1792–1799. The cruciform dynamic vibration absorber.
2. H. Yamaguchi and H. Saito 1984 *Earhquake Engineering and Structural Dynamics* **12**, 467–479. Vibrations of beams with an absorber consisting of a viscoelastic solids and beam.
3. K. Nagaya and H. Kojima 1984 *ASME*, *Journal of Dynamic Systems*, *Measurement and Control* **106**, 46–51. On a magnetic damper consisting of a circular magnetic flux and a conductor of arbitrary shape (Part 1:Derivation of damping coefficients)
4. K. Nagaya 1984 *ASME*, *Journal of Dynamic Systems*, *Measurement and Control* **106**, 52–55. On a magnetic damper consisting of a circular magnetic flux and a conductor of arbitrary shape (Part 2: applications and numerical results).
5. D. H. Consalves, R. D. Neilson, A. D. S. Barr 1993 *Proceedings of the Institution of Mechanical Engineers*, *Part C*, *Journal of Mechanical Engineering Science* **207**, 363–374. The dynamics and design of a non-linear vibration absorber.
6. S. W. Shaw and S. Wiggins 1988, *Journal of Applied Mechanics* **55**, 952–958. Chaotic motions of a torsional vibration absorber.
7. J. Lee 1990, *Earthquake Engineering and Structural Dynamics* **19**, 1209–1218. Optimal weight absorber designs for vibrating structures exposed to random excitations.
8. K. Nagaya and Y. Li 1998, *Journal of Acoustical Society of America* **104**, 1466–1473. Method for reducing sound radiated from structures using vibration absorbers optimized with a neural network.

9. M. Venugopal 1990, *Marine Technology*, 42–46. A toroidal hydrodynamic absorber for damping low frequency motions of fixed and floating offshore platforms.
10. G. F. Topinka 1986 *Hydruarics and Pneumatics* **39**, 14. Shock absorber, used in tension, solves cushioning, valving problems.
11. R. E. Mondy 1985, *Power* **129**, 51–52. Absorber stops elusive multi-stage-pump vibrations.
12. T. Szirtes 1989 *Machine Design* **61**, 66. Choosings the right shock absorber.
13. G. Lee, J. Gina, G. Ahmad and G. H. Lucas 1997 *Journal of Structural Engineering* **123**, 499–504. Integrated passive/active vibration absorber for multistory buildings.
14. N. Patten William, L. Sack Ronald and Q. He 1996, *Journal of Structural Engineering* **122**, 187–192. Controlled semiactive hydraulic vibration absorber for bridges.
15. M. Bruner Anne, W. K. Belvin and G. Horta Lucas 1992 *Journal of Guidance, Control, and Dynamics* **15**, 1253–1257. Active vibration absorber for CSI evolutionary model: design and experimental results.
16. N. Olgac, B. Holm-hansen 1995 *ASME, Journal of Dynamic Systems, Measurement and Control* **117**, 513–519. Tunable active vibration absorber; the delayed resonator.
17. J. Q. Sun, M. A. Norris and M. R. Jolly 1995 *The 50th Anniversary of ASME Journal of Vibration and Acoustics and Journal of Mechanical Design* **117**, 234–242. Passive, adaptive and active tuned vibration absorbers—a survey.
18. Y. Tokita and M. Morimuara 1992 *Vibration Control Handbook*, 249–281, Japan: Fuji Techno System.
19. K. Nagaya and L. Li 1997 *Journal of Sound and Vibration* **208**, 289–298. Control of sound noise radiated from a plate using dynamic absorbers under the optimization by neural network.
20. Y. K. Lin 1967 *Probabilistic Theory of Structural Dynamics*. New York; R.E. Krieger Publishing Company.
21. J. Q. Sun 1994 *Journal of Sound and Vibration* **185**, 827–843. Vibration and sound radiated of nonuniform beams.